

BRIEF REPORT



Anti-GD2 antibody and Vorinostat immunocombination therapy is highly effective in an aggressive orthotopic neuroblastoma model

Renske J. E. van den Bijgaart^a, Michiel Kroesen^b, Ingrid C. Brok^a, Daphne Reijnen^c, Melissa Wassink^a, Louis Boon^d, Peter M. Hoogerbrugge^e, and Gosse J Adema^a

^aRadiotherapy & Oncology Laboratory, Department of Radiation Oncology, Radboud University Medical Center, Nijmegen, The Netherlands; ^bHolland Proton Therapy Center, Delft, The Netherlands; ^cCentral Animal Laboratory, Radboud University Medical Center, Nijmegen, The Netherlands; ^dBioceros, Utrecht, The Netherlands; ^eDepartment of Pediatric Oncology, Princess Máxima Center for Pediatric Oncology, Utrecht, The Netherlands

ABSTRACT

Neuroblastoma is a childhood malignancy and in the majority of patients, the primary tumor arises in one of the adrenal glands. Neuroblastoma cells highly express the disialoganglioside GD2, which is the primary target for the development of neuroblastoma immunotherapy. Anti-GD2 mAbs have shown clinical efficacy and are integrated into standard treatment for high-risk neuroblastoma patients. We previously reported synergy between the HDAC inhibitor Vorinostat and anti-GD2 mAbs in a heterotopic, subcutaneous growing neuroblastoma model. Additionally, we have previously developed an orthotopic intra-adrenal neuroblastoma model showing more aggressive tumor growth. Here, we report that anti-GD2 mAb and Vorinostat immunocombination therapy is even more effective in suppressing neuroblastoma growth in the aggressive orthotopic model, resulting in increased animal survival. Intra-adrenal tumors from mice treated with Vorinostat were highly infiltrated with myeloid cells, including macrophages, displaying increased MHCII and Fc-receptor expression. Collectively, these data provide a strong rationale for clinical testing of anti-GD2 mAbs with concomitant Vorinostat in neuroblastoma patients.

ARTICLE HISTORY

Received 17 March 2020
Revised 26 August 2020
Accepted 27 August 2020

KEYWORDS

Neuroblastoma; orthotopic; immunotherapy; anti-GD2 mAb therapy; histone deacetylase inhibitor

Introduction


Neuroblastoma is the most common extra-cranial solid tumor in pediatric oncology accounting for 12% of cancer-related deaths in children younger than 15 y.¹ Neuroblastoma arises from the aberrant growth of neural crest progenitor cells of the developing sympathetic nervous system. In approximately 65% of patients the primary tumor arises in one of the adrenal glands.² Neuroblastoma cells uniformly and highly express the disialoganglioside GD2, a tumor-associated carbohydrate antigen. In healthy tissues, GD2 expression is weak and restricted to neurons, skin melanocytes, and peripheral pain fibers.²⁻⁴ The preferential expression of GD2 by neuroblastoma cells makes it an ideal target for immunotherapy.⁵

Therefore, GD2 has been the primary target for the development of immunotherapeutic monoclonal antibodies (mAbs). Anti-GD2 mAbs effectively mediate lysis of neuroblastoma cells via antibody-dependent cell-mediated cytotoxicity (ADCC) as well as complement-dependent cytotoxicity.² Fc-receptor expressing immune cells have been implicated as the main effector cells in the clinical response following anti-GD2 mAb therapy.^{6,7} Anti-GD2 mAbs, including dinutuximab, proved to be safe and effective in clinical trials and are incorporated into standard of care for high-risk neuroblastoma patients.⁴ The standard treatment for high-risk neuroblastoma patients therefore now includes chemotherapy, surgical resection, high-dose chemotherapy with autologous hematopoietic

stem cell transplantation, external beam radiotherapy, the differentiating agent isotretinoin and immunotherapy with anti-GD2 mAbs plus cytokines.^{8,9} Although the prognosis of high-risk neuroblastoma patients has improved over the last decades, the long-term survival still remains poor.¹⁰

The immunosuppressive tumor microenvironment hampers immune cell function and limits the success of cancer (immuno)therapies.¹¹ Neuroblastomas are highly infiltrated with suppressive myeloid cells, including tumor-associated macrophages, which are associated with an adverse prognosis.¹² Counteracting the immunosuppressive microenvironment is an important step in improving cancer immunotherapy. Epigenetic modifying drugs can cause tumor cells to re-express or release otherwise downregulated antigens, thereby enabling enhanced detection of tumor cells by the immune system. Preclinical studies have shown that epigenetic modifying drugs are able to modulate the immunosuppressive tumor microenvironment by reducing suppressive immune cells, such as myeloid-derived suppressor cells (MDSCs), or impairing suppressive functions of regulatory T cells.^{13,14} Therefore, epigenetic regulators are promising therapeutic targets also in neuroblastoma. Histone deacetylases (HDAC) are a group of epigenetic modifiers that remove acetyl groups from histone and non-histone proteins and HDAC inhibitors were shown to induce cell cycle arrest and differentiation in neuroblastoma and other cancers.¹⁵⁻¹⁷ Preclinical data have demonstrated the efficacy of various HDAC inhibitors as single-agent

CONTACT Gosse J Adema  gosse.adema@radboudumc.nl  Radiotherapy & Oncology Laboratory, Department of Radiation Oncology, Radboud University Medical Center, Nijmegen, The Netherlands

 Supplemental data for this article can be accessed on the [publisher's website](#).

© 2020 RadboudUMC. Published with license by Taylor & Francis Group, LLC.

This is an Open Access article distributed under the terms of the Creative Commons Attribution-NonCommercial License (<http://creativecommons.org/licenses/by-nc/4.0/>), which permits unrestricted non-commercial use, distribution, and reproduction in any medium, provided the original work is properly cited.

anticancer therapeutics, but the greatest effects were observed when HDAC inhibitors are used in combination with other therapies.^{13,18} We have recently reported that the pan-HDAC inhibitor Vorinostat synergized with anti-GD2 mAb therapy in a subcutaneous transplantable TH-MYCN neuroblastoma model.^{13,19} This model closely resembles high-risk human neuroblastoma, including endogenous expression of the tumor-associated antigen GD2.¹⁹ Vorinostat enhanced GD2 expression by the neuroblastoma cells and synergized with anti-GD2 mAb therapy in reducing neuroblastoma growth. Vorinostat created a more permissive tumor microenvironment for tumor-directed mAb therapy, by increasing the number of potential effector cells expressing high levels of Fc-receptors.^{13,20}

Orthotopic models are known to better simulate clinical disease compared to heterotopic models, by the better reflection of tumor biology and tumor microenvironment. We recently developed an orthotopic transplantable TH-MYCN neuroblastoma model, by injecting MYCN transgenic 9464D neuroblastoma cells intra-adrenally using microsurgery in C57Bl/6 mice.²¹ Intra-adrenal neuroblastomas grow faster and more aggressively compared to their subcutaneous counterparts. Furthermore, intra-adrenal neuroblastoma exhibited a more immunosuppressive tumor microenvironment, as tumor-infiltrating macrophages were highly abundant and expressed lower levels of MHCII.²¹

In this study, we investigated whether the combination of anti-GD2 mAb and HDAC inhibitor Vorinostat would be effective in the more aggressive orthotopic model of neuroblastoma. We could demonstrate that immunocombination therapy is highly effective in suppressing aggressive orthotopic neuroblastoma growth, resulting in increased survival of mice. We were able to confirm that Vorinostat treatment altered the immune composition of orthotopic tumors, inducing a strong increase in the percentage of total leukocytes. Specifically, tumor-infiltrating myeloid cells were affected by Vorinostat treatment, as shown by an increase in the percentage of F4/80^{high} macrophages, CD11c^{high}MHCII^{high} dendritic cells and Ly6C^{high}Ly6G^{neg} monocytes. Overall, myeloid cells displayed a more activated phenotype with significantly higher expression of the activation markers MHCII and FcRγI after Vorinostat treatment. Collectively, these data imply further testing of epigenetic modulators with immunotherapy in general and confirm a strong rationale for clinical testing of anti-GD2 mAbs and Vorinostat immunocombination therapy in neuroblastoma patients specifically.

Materials and methods

Animals and cell lines

Six- to eight-week-old female C57Bl/6 J wild-type mice were purchased from Charles River (Sulzfeld, Germany). B6(Cg)-Tyr^{c-2J}/J were purchased from The Jackson Laboratory (Bar Harbor, ME). These mice carry a mutation in the tyrosinase gene, resulting in the absence of pigment. Animals were held under specified pathogen-free conditions in the Central Animal Laboratory (Nijmegen, the Netherlands) and *ad libitum* access to food and water. All experiments were performed

according to the guidelines for animal care of the Nijmegen Animal Experiments Committee. The transgenic cell line 9464D was derived from spontaneous tumors from TH-MYCN transgenic mice on C57Bl/6 background and was a kind gift from Dr. Orentas (National Institutes of Health, Bethesda, MD). 9464D-luc cells were generated as described previously and were cultured in Dulbecco's modified Eagle's medium – GlutaMAX (Gibco) containing 10% Fetal Bovine Serum (FBS, Greiner Bio-One), 1% non-essential amino acids (Gibco), 1% antibiotic–antimycotic (Gibco), 50 μM β-mercaptoethanol (Sigma Aldrich) and 1 mg/ml G418 (Gibco).²¹

Intra-adrenal injection of 9464D-luc cells

For intra-adrenal tumor growth, 1×10^6 9464D-luc cells were injected intra-adrenally. Viability of tumor cells before injection exceeded 95% as was determined by trypan blue staining. For intra-adrenal injections, microsurgery was performed by a skilled biotechnician. Institutional protocols and guidelines were adhered to for the delivery of anesthesia and analgesia. Briefly, a dorsal incision was made right lateral to the spinal cord, and the retroperitoneum was accessed. The kidney and adrenal gland were located, and using a 0.3-ml Becton Dickinson (BD) Micro-Fine™ needle, 1×10^6 9464D-luc cells were injected in a volume of 30 μl phosphate-buffered saline (PBS) into the adrenal gland. Using sutures, the retroperitoneum and skin were closed. Within 7 d, sutures could be removed and wounds were fully healed without any signs of inflammation.

Monitoring tumor growth by bioluminescence

Tumor growth of 9464D-luc tumors at adrenal sites was monitored over time using bioluminescence. The dorsal skin of the mice was shaved before each measurement. Mice were injected intraperitoneally (i.p.) with 150 μg D-Luciferin (PerkinElmer, MA) in 200 μl PBS and anaesthetized using isoflurane. Ten minutes after injection of D-Luciferin, mice were imaged using an *in vivo* imaging system (IVIS) Lumina (Xenogen, Alameda, CA) camera by taking consecutive 1 s to 2 min imaging frames.

Anti-GD2 mAb and Vorinostat treatment *in vivo*

All mice were randomized just before treatment initiation. Anti-GD2 mAb or isotype control treatment started on day 3 following tumor inoculation by i.p. injection of 200 μg mAb and was repeated twice weekly. Vorinostat was purchased from SelleckChem (Houston, TX). For *in vivo* use, Vorinostat was dissolved to a final concentration of 50 mg/ml in DMSO/PBS (2:1). Vorinostat treatment started on day 7 following tumor inoculation by injecting 150 mg/kg Vorinostat or vehicle control i.p. for 3 consecutive days and was repeated every week. To study the effect of anti-GD2 mAb, Vorinostat or combination therapy on intra-adrenal neuroblastoma growth and subsequent tumor microenvironment analysis, the treatment schedule was repeated for 4 weeks (end point at day 37). When mice reached the humane end point earlier, tumors were excised and weighted. To study tumor growth and survival in

B6(Cg)-Tyr^{c-2J}/J mice, the same schedule was used for a total of 8 weeks (treatment ceased at day 57). The researcher was not blinded to treatment groups during the experiments.

Reagents and antibodies

Purified anti-CD16/CD32 (2.42 G), anti-CD45.2-biotin (104), anti-CD45.2-FITC (104), anti-CD11c-APC (HL3), anti-Ly6C-APCCy7 (AL-21) and PE-conjugated goat anti-mouse Ig were purchased from BD Biosciences (BD Pharmingen). Anti-CD11b-A700 (M1/70), anti-F4/80-PECy7 (BM8), anti-MHCII-PerCP (M5/114.15.2), anti-CD64-PE (X54-5/7.1), anti-CD16/CD32-APC (93), anti-MHCII-biotin (M5/114.15.2), anti-CD64-biotin (X54-5/7.1), anti-Ly6G-PECy7 (1A8), anti-CD4-PerCP (RM4-5) and streptavidin-PerCP were purchased from Biolegend (San Diego, CA). Anti-F4/80-biotin (BM8), anti-CD25-APC (PC61.5), anti-FoxP3-PECy7 (FJK-16s) and anti-MHCII-PE (M5/114.15.2) were obtained from eBioscience (San Diego, CA). Anti-CD8-A700 (53-6.7) was purchased from Exbio (Czech Republic). Goat anti-rat Alexa Fluor 555 was obtained from Invitrogen (Carlsbad, CA). Donkey anti-goat HRP was obtained from Santa Cruz Biotechnology (Santa Cruz, CA). Mouse anti-GD2 antibody (clone 14G2a) was purified from a hybridoma cell line (obtained from Dr. Reisfeld, Scripps, La Jolla, CA).²² Total mouse IgG control Ab was obtained from Jackson ImmunoResearch (West Grove, PA).

Generation of single-cell suspensions of tumors

Tumors were excised at the end of the experiment and mechanically dissociated and enzymatically digested with 1 mg/mL collagenase Type III (Worthington) and 30 µg/mL DNase type I (Roche) for 1 h at 37 °C. EDTA was added to a final concentration of 1 mM and single-cell suspensions were made by passing the tumor fragments over 100 µm cell strainers.

Antibodies and flow cytometry

After single-cell suspensions were made, cells were incubated for 10 min with PBA containing anti-CD16/CD32 Fc-receptor blocking antibody (2.42 G), after which cells were incubated with fluorescent antibodies directed against surface molecules for 30 min at 4°C. Samples were not blocked when Fc-receptor expression was determined. Cells were washed twice with PBA and measured on a CyAn ADP flow cytometer (Beckman Coulter, Fullerton, CA) and data were analyzed using FlowJo software (Tree Star Inc., Ashland, OR).

Immunohistochemistry

Frozen tumor tissues were sectioned into 5 µm sections. Cryosections were fixed with acetone at 4°C for 10 min. Sections were air-dried and subsequently hydrated by in PBS for 5 min at room temperature. Endogenous peroxidase activity was quenched with 0.3% H₂O₂ in methanol for 10 min at room temperature. Anti-CD45.2-biotin, anti-F4/80-biotin, anti-MHCII-biotin, anti-CD64-biotin and purified anti-CD16/CD32 were diluted in primary antibody diluent (Bio-Rad)

and incubated on the tissue for 45 min at 37°C. Sections were washed, and the sections that were incubated with the purified anti-CD16/CD32 were subsequently incubated with Goat anti-Rat Alexa Fluor 555 for 45 min at 37°C, subsequently washed and incubated HRP-conjugated donkey anti-goat for 45 min at 37°C. Sections were washed and the antibody was detected using the ABC Vectastain kit and DAB, 3,3'-Diaminobenzidine (Vector Laboratories, Burlingame, CA). We performed counterstaining with Hematoxylin (DAKO, Agilent, Santa Clara, CA), dehydrated the sections and mounted with Histochoice mounting media (VWR International) and a coverslip. Images were acquired with a Axioimager D2 microscope (Carl Zeiss GmbH, Oberkochen, Germany) at 10x magnification.

Statistics

Comparisons between multiple groups were made using one-way analysis of variance (ANOVA) followed by Bonferroni's correction. Kaplan-Meier survival curves were analyzed with a log-rank test using Prism 5 software (GraphPad Inc, La Jolla, CA, USA). *P*-values <0.05 were considered statistically significant (*p* < .05 *, *p* < .01 **).

Results

Anti-GD2 mAb and Vorinostat also suppress intra-adrenal neuroblastoma growth

Orthotopic neuroblastomas in the adrenal gland grow faster compared to their subcutaneous counterparts and exhibit a more immunosuppressive phenotype.²¹ Previously, we reported that anti-GD2 mAb and Vorinostat therapy, initiated at day 8 and day 14, respectively, synergized in the treatment of a subcutaneous neuroblastoma model.¹³ These data prompted us to investigate the effect of anti-GD2 mAbs and Vorinostat immunocombination therapy in the more aggressive orthotopic intra-adrenal neuroblastoma model. Mice bearing intra-adrenal luciferase-expressing 9464D neuroblastomas were treated with anti-GD2 mAbs, Vorinostat or the combination of both. During therapy, tumor growth was monitored using bioluminescent imaging. Because of the aggressive intra-adrenal neuroblastoma growth, treatment was initiated earlier compared to the subcutaneous model. Anti-GD2 mAb therapy was initiated on day 3 following tumor inoculation and was repeated twice weekly for four weeks. Vorinostat treatment was started on day 7 and consisted of daily i.p. injections (150 mg/kg) administered for 3 consecutive days and this treatment schedule was repeated weekly for four weeks (Figure 1a). Bioluminescent imaging showed that anti-GD2 mAb treatment alone had minimal impact on tumor growth relative to isotype control, whereas Vorinostat monotherapy and in combination with anti-GD2 mAbs reduced tumor growth compared to the vehicle control (Suppl. Figure S1).

At day 37 or earlier, mice were sacrificed and tumor weight was determined. Tumor weights in the Vorinostat treated group were significantly lower compared to the isotype group (Figure 1b). Combination therapy with anti-GD2 mAbs and Vorinostat significantly reduced tumor weight relative to anti-

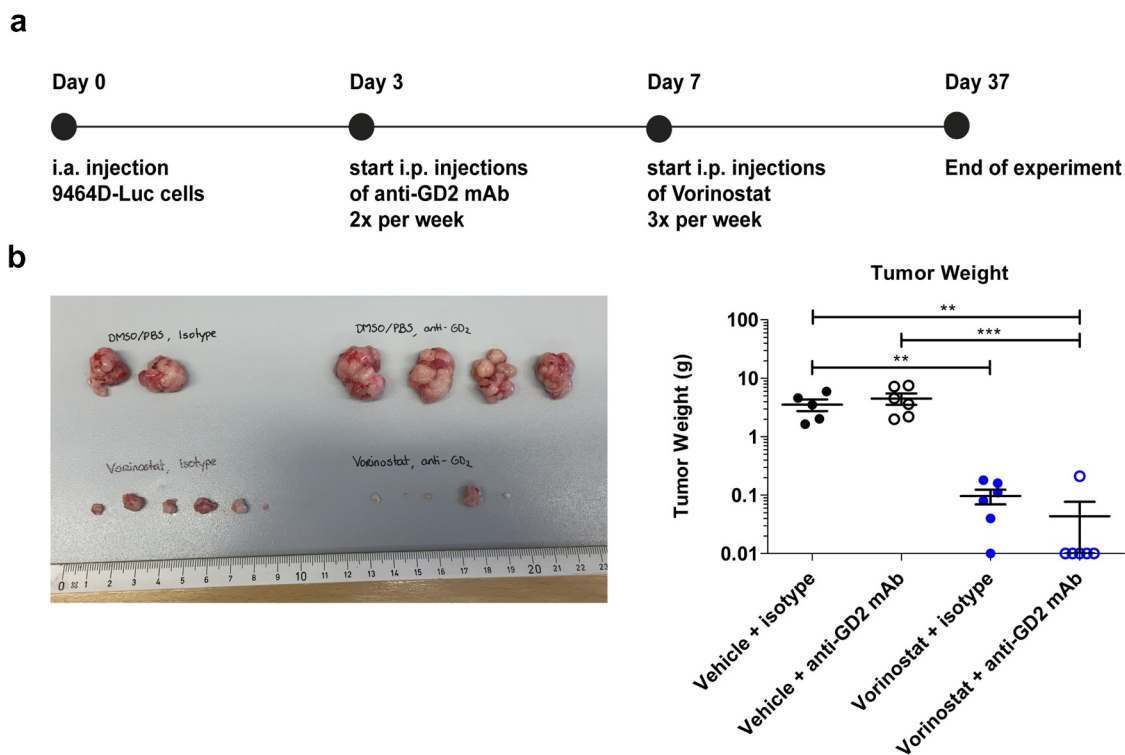


Figure 1. Immunocombination therapy using anti-GD2 mAb and Vorinostat dramatically reduces intra-adrenal neuroblastoma tumor weight. (a) Diagram shows the treatment schedule for immunocombination therapy using anti-GD2 mAb and Vorinostat. Mice were inoculated intra-adrenally with 1×10^6 9464D-luc cells on day 0. Anti-GD2 mAb therapy (200 μ g per injection, i.p.) was initiated on day 3 and repeated two times per week. Vorinostat therapy (150 mg/kg) was initiated on day 7 and given for 3 consecutive days and this scheme was repeated weekly for four weeks. Tumor growth was monitored using bioluminescent imaging. (b) Left; picture of tumors that were excised at day 37 or when mice were sacrificed earlier (Isotype $n = 5$, anti-GD2 mAb $n = 6$, Vorinostat $n = 6$, anti-GD2 mAb + Vorinostat $n = 6$).

GD2 mAb therapy alone and isotype control (Figure 1b). Strikingly, in the combination treatment group, 5 out of 6 mice did not have a visible tumor and the adrenal gland weight was determined (Figure 1b). These initial results demonstrated that the combination of anti-GD2 mAbs and Vorinostat dramatically reduced tumor growth in the highly aggressive orthotopic neuroblastoma model.

Vorinostat alters the tumor microenvironment composition

Next to tumor weight measurements, we assessed the presence and phenotype of immune cells in the tumor microenvironment of these neuroblastoma tumors following the different treatments by flow cytometry using the gating strategy outlined in Suppl. Figure 2. Since mice in the anti-GD2 mAb with Vorinostat combination treatment group had barely any tumor present, we could not include these tumors in the analysis. Tumors from mice treated with Vorinostat contained significantly more immune cells, as defined by the leukocyte marker CD45.2 (Figure 2a). The percentage of myeloid cells, as defined by CD11b, was not different between the treatment modalities (Figure 2b). Analysis of the tumor-infiltrating myeloid cells showed a significant increase in the percentage of F4/80^{high} macrophages as well as CD11c^{high}MHCII^{high} dendritic cells upon Vorinostat treatment (Figure 2c,d). The markers Ly6C and Ly6G were used to define monocytes and neutrophils, respectively. The percentage of Ly6C^{high}Ly6G^{neg} monocytes was enhanced, whereas the

percentage of Ly6C^{dim}Ly6G^{high} neutrophils was decreased in Vorinostat treated tumors (Figure 2e,f). The Ly6C^{high}Ly6G^{neg} monocytes detected upon Vorinostat treatment expressed significantly higher levels of MHCII, highly indicative of an immunostimulatory rather than an MDSC immunosuppressive phenotype (Figure 2g). No significant differences were observed in T cell infiltration (Figure 2h). NK and B cells are scarcely present in the neuroblastoma microenvironment and unaltered by treatment (data not shown).

Overall, myeloid cells in the Vorinostat treated tumors displayed a more activated phenotype with significantly higher expression of the activation markers MHCII and FcRyI (Figure 2i, j). FcRyII/III expression was slightly increased on the tumor-infiltrating myeloid cells (Figure 2k). Next, we analyzed the expression of GD2 in the treated intra-adrenal growing tumors. In line with our findings in subcutaneous growing tumors, Vorinostat treatment enhanced expression of the tumor antigen GD2 (Figure 2l). These results indicate that Vorinostat especially increases the presence and alters the phenotype of myeloid cells in neuroblastomas and creates a more immune permissive tumor microenvironment for mAb directed therapy.

Next, we investigated the spatial distribution of tumor-infiltrating immune cells by immunohistochemistry. Macrophage activation markers MHCII, FcRyI and FcRyII/III were included and stainings were performed on consecutive sections. Using CD45.2 and F4/80 staining, we observed numerous tumor-infiltrating leukocytes and macrophages in the neuroblastoma microenvironment, respectively. Macrophages infiltrated the

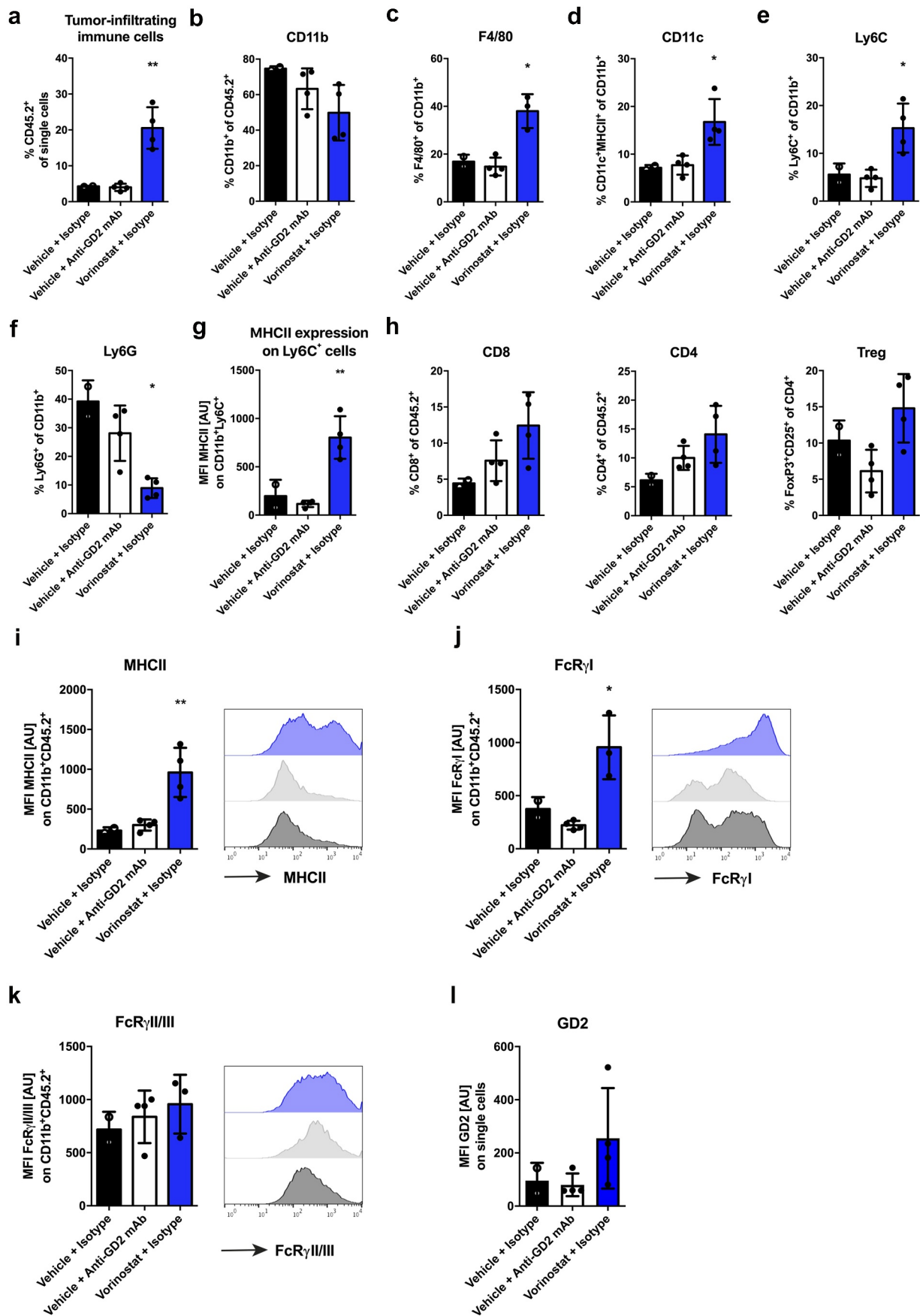


Figure 2. Vorinostat treated tumors are highly infiltrated with leukocytes, expressing high levels of MHCII and Fc-receptors. Mice bearing intra-adrenal 9464D tumors were treated with isotype, anti-GD2 mAb or Vorinostat according to schedule of Figure 1a. At day 37 tumors were excised and single-cell suspension were made of available tumors. (a-f) Bar graphs show mean percentages \pm SD of tumor-infiltrating CD45.2⁺ immune cells (a), CD11b⁺ myeloid cells (b), F4/80^{high} macrophages (c), CD11c^{high}MHCII^{high} dendritic cells (d), Ly6C^{high}Ly6G^{neg} monocytes (e) and Ly6C^{dim}Ly6G^{high} granulocytes (f). (g) Bar graphs show mean fluorescent intensity (MFI) \pm SD of MHCII on Ly6G^{neg}Ly6C^{high} monocytes. (h) Bar graphs show mean percentages \pm SD of tumor-infiltrating CD8⁺ T cells, CD4⁺ T cells and CD25⁺FoxP3⁺ regulatory T cells. (i-k) Bar graphs show MFI \pm SD with representative histogram of MHCII (i), FcRγI (j) and FcRγII/III (k) on CD11b⁺ myeloid cells. (l) Bar graphs show mean MFI \pm SD of GD2 on single cells. (Isotype n = 2, anti-GD2 mAb n = 4, Vorinostat n = 3–4).

neuroblastoma as diffusely scattered cells. In the Vorinostat treated mice, we observed more densely infiltrated areas with high accumulation of leukocytes and macrophages (Figure 3a,b). Furthermore, macrophages in Vorinostat treated tumors expressed high levels of MHCII and Fc-receptors (Figure 3c-e). Altogether, the immunohistochemical analysis matches the immune cell infiltration and marker expression as shown by flow cytometry.

Anti-GD2 mAb plus Vorinostat combination therapy enhances survival

The black fur and pigment of C57Bl/6 mice can significantly block the luminescent signal coming from the tumor. Therefore, the tumor growth experiment described

above was repeated using C57Bl/6 albino mice that lack pigmentation in fur. Treatment schedule in these mice was similar as the wildtype C57Bl/6 mice, although treatment was continued for eight weeks (Figure 4a). The combination of anti-GD2 mAb with Vorinostat therapy resulted in a strong reduction of tumor growth (Figure 4b). After the treatment was ceased at day 57, the mean tumor volume in the combination treatment group started to increase (Figure 4b). Although tumors ultimately relapsed, the combination treatment significantly increased the median survival from 37 d to 65 d (Figure 4c). In conclusion, these data show that the combination of anti-GD2 mAb-based immunotherapy and Vorinostat results in a strong suppression of tumor growth and improved survival in this aggressive orthotopic neuroblastoma model.

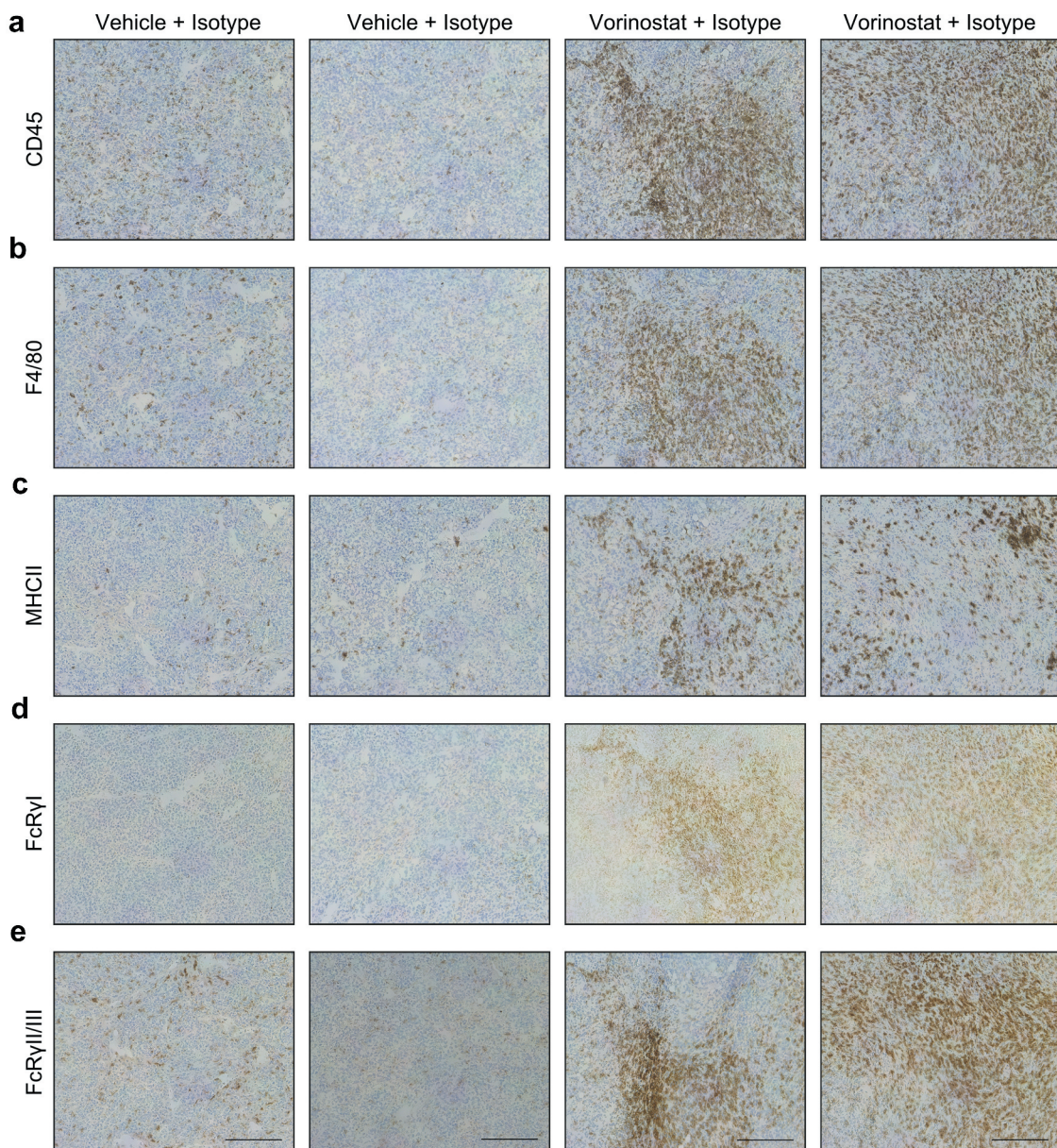


Figure 3. Immunohistochemical detection of CD45.2, F4/80, MHCII, FcR γ I and FcR γ II/III positive cells in neuroblastoma tumor sections. Mice bearing intra-adrenal 9464D tumors were treated with isotype, anti-GD2 mAb or Vorinostat according to schedule of Figure 1a. At day 37 tumors were excised and available tumors were snap frozen. Immunohistochemistry staining for CD45.2 (a), F4/80 (b), MHCII (c), FcR γ I (d) and FcR γ II/III (e) in two representative isotype control and Vorinostat treated mice.

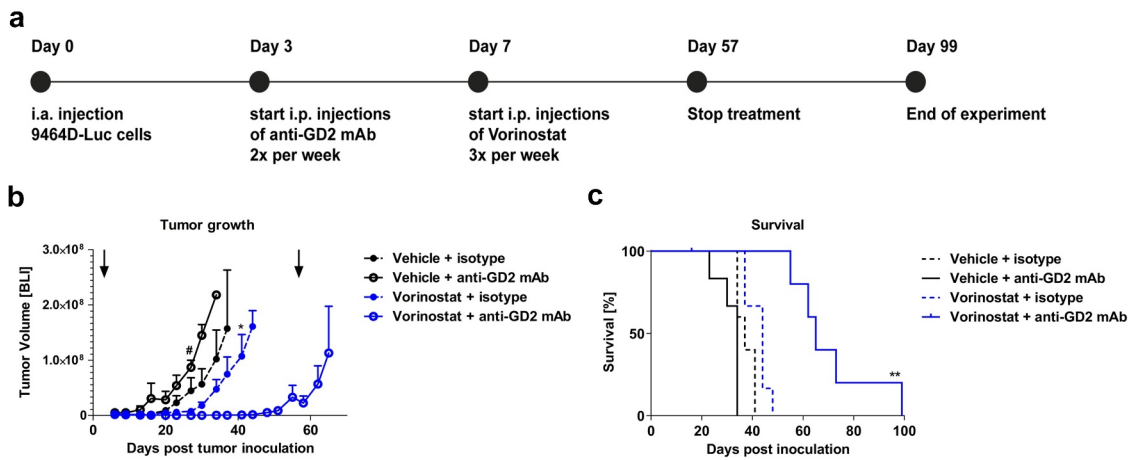


Figure 4. Combined treatment with anti-GD2 mAbs and Vorinostat increases survival of intra-adrenal tumor-bearing C57Bl/6 albino mice. (a) Diagram shows the treatment schedule for immunocombination therapy using anti-GD2 mAb and Vorinostat. C57Bl/6 albino mice were inoculated intra-adrenally with 1×10^6 9464D-luc cells on day 0. Anti-GD2 mAb therapy was initiated on day 3 and repeated two times per week. Vorinostat therapy was initiated on day 7 and given for 3 consecutive days and this scheme was repeated weekly for eight weeks (until day 57), where after treatment was stopped. Tumor growth was monitored using bioluminescent imaging. (b) Intra-adrenal neuroblastoma tumor growth was monitored twice weekly using bioluminescence. Quantification of the bioluminescent count represents tumor growth. Arrows indicate start and end of treatment regimen. Mean tumor volumes of each treatment group are depicted (* $p < .05$ for anti-GD2 vs. Vorinostat + anti-GD2 mAb) (* $p < .05$ for Vorinostat vs. Vorinostat + anti-GD2 mAb). (c) Kaplan-meier curves show survival percentages of mice inoculated intra-adrenally with 9464D-luc cells receiving isotype, anti-GD2 mAb, Vorinostat or anti-GD2 mAb + Vorinostat treatment ($n = 6$ per group, one mouse in the isotype group was excluded from the analysis due to a water kidney).

Discussion

In this study, we report that anti-GD2 mAb and Vorinostat immunocombination therapy elicits a strong anti-tumor effect in a highly aggressive orthotopic intra-adrenal neuroblastoma mouse model. Vorinostat monotherapy significantly reduced intra-adrenal tumor weight. Strikingly, 5 out of 6 mice treated with the combination therapy of anti-GD2 mAb and Vorinostat barely had any tumor present in the adrenal gland. We confirmed that Vorinostat treatment has a profound effect on the neuroblastoma microenvironment which contained significantly more immune cells. Specifically, tumor-infiltrating myeloid cells were affected by Vorinostat treatment, as shown by an increase in the percentage of F4/80^{high} macrophages, CD11c^{high}MHCII^{high} dendritic cells and Ly6C^{high}Ly6G^{neg} monocytes, and a decrease in the abundance of Ly6C^{dim}Ly6G^{high} neutrophils. Overall, myeloid cells displayed a more activated phenotype with significantly higher expression of the activation markers MHCII and FcRγI after Vorinostat treatment. No significant differences were observed in T cell, B cell and NK cell infiltration in the neuroblastoma microenvironment following therapy. Using albino C57Bl/6 mice and luciferase reporting neuroblastoma cells, we demonstrated that combination treatment strongly reduced tumor growth and significantly increased survival. The fact that we observed remarkable anti-tumor activity in the aggressive tumor model is encouraging. Orthotopic models better reflect the complex organ-specific aspects of tumor biology as well as the tumor microenvironment.²³ The latter is of high importance, as the local tumor microenvironment can influence tumor biology and progression, as well as immune responses to cancer upon therapy.

In this study, using the highly aggressive intra-adrenal neuroblastoma model, anti-GD2 mAb therapy was initiated on day 3 following tumor inoculation which is earlier compared to the

subcutaneous model where mAb therapy was initiated on day 8. This treatment regimen was chosen as the intra-adrenal neuroblastomas grow faster compared to their subcutaneous counterparts. However, in both studies, treatment was initiated with anti-GD2 mAbs followed by Vorinostat therapy as studies suggested that immune activation preceding HDAC inhibitor therapy results in better immune cell survival and function.²⁴

Tumor-infiltrating macrophages are more abundant in intra-adrenal neuroblastomas and show a more immunosuppressed phenotype with lower MHCII expression levels compared to their subcutaneous equivalents.²¹ Converting these large amounts of pro-tumoral macrophages into cells capable of performing anti-GD2 mAb mediated ADCC could explain the highly effective anti-tumor effect observed. Furthermore, the percentage of Ly6C^{high}Ly6G^{neg} monocytes was enhanced upon Vorinostat treatment, whereas the abundance of Ly6C^{dim}Ly6G^{high} cells decreased. Monocytic MDSCs and polymorphonuclear MDSCs are also identified by the expression of Ly6C and Ly6G, respectively, and discrimination of these MDSCs subsets from bonafide monocytes and neutrophils is challenging.²⁵ The Ly6C^{high}Ly6G^{neg} monocytes detected in the Vorinostat treated tumors expressed significantly higher levels of MHCII, highly indicative of an inflammatory monocyte phenotype with immunostimulatory properties rather than a phenotype corresponding to MDSC. Functional characterization would be essential to further validate these findings. Although our study suggests that Fc-receptor expressing myeloid cells are the main effector cells in the efficacy of Vorinostat plus anti-GD2 mAb therapy, we cannot exclude that other Fc-receptor expressing cells, such as NK cells, also participate. We previously reported that NK cells are involved in the natural immune response against 9464D tumors.¹⁹ Whether Fc-receptor expression on NK cells is altered upon Vorinostat treatment and affects treatment outcome remains to be

elucidated, preferentially by detecting Fc-receptor protein expression using flow cytometry.

Although our results suggest that the combination therapy is more effective in the orthotopic intra-adrenal neuroblastoma model, we cannot directly compare the subcutaneous with the orthotopic model, as we did not perform a comparative study. Nevertheless, based on our previous work in the subcutaneous model, tumors in mice from the combination therapy group started to appear and grow out at day 45,¹³ while in the more aggressively orthotopic model there is still no tumor detected at this time point. Even though the combination of anti-GD2 mAb with Vorinostat therapy resulted in a synergistic reduction of tumor growth, tumors ultimately relapsed when treatment was ceased. It is plausible that the combination therapy besides direct cytotoxic effect also exerts cytostatic effects which could be responsible for the immediate outgrowth of tumor cells after discontinuation of therapy. As alternative explanation, neuroblastoma cells that are still residing within the adrenal gland could be present in a dormant state or have downregulated the tumor antigen GD2. This latter explanation seems less likely as GD2 expression is rarely lost after treatment with anti-GD2 mAb.^{26,27} The presence of resistant neuroblastoma cells in this model, a well-known clinical problem, allows for further studies into the mechanisms of tumor therapy evasion in the future.

Tumor-associated macrophages often have net pro-tumor effects,²⁸ but their embedded location and plasticity provides a rationale for therapeutic strategies to turn them into anti-tumor immune cells. Interestingly, a selective class IIa HDAC inhibitor, TMP195, was shown to modulate macrophage phenotype and induced recruitment and differentiation of highly phagocytic and stimulatory macrophages within tumors. Thereby, TMP195 reduced tumor growth and pulmonary metastases in a preclinical breast cancer model.²⁹ Further research is needed to unravel the precise mechanisms underlying macrophage reprogramming and recruitment after HDAC inhibition. Furthermore, it would be interesting to study the effect of class or isotype selective HDAC inhibitors, to prevent potential side-effects of the pan-HDAC inhibitors.

Fc-receptor expressing immune effector cells are highly important for the clinical response following tumor-directed mAb therapy, including anti-GD2 mAb therapy. Anti-GD2 mAb alone did not significantly alter the tumor microenvironment nor inhibited tumor growth. This is in line with observations in neuroblastoma patients, where there is a need to activate the immune system with cytokines, including IL-2 and GM-CSF, to obtain effective anti-GD2 therapy.⁹ The combination with Vorinostat may, similarly to cytokines, enable activation of the immune system and thereby work synergistically with the anti-GD2 mAb therapy. Besides its targeting efficacy to direct immune-mediated killing, GD2 is also an ideal target for tumor-selective delivery of radioisotopes or immune stimuli. Interestingly, anti-GD2 mAb conjugates, like anti-GD2 mAb coupled to IL-2, have been generated and show clinical efficacy.³⁰ Nevertheless, a major side effect is pain, thought to be a consequence of complement activation, which remains a clinical burden.^{9,31} There are efforts to optimize the efficacy of anti-GD2 mAb-based (combination) therapies while reducing its side effects, for example, by using CAR

T cells or carbohydrate-based vaccines.^{32,33} Also, it has been suggested that O-acetyl-GD2 is specifically expressed on neuroblastoma cells, but not on peripheral nerves.³⁴ The used 14G2a anti-GD2 mAb in this study recognizes both GD2 and the O-acetylated form of GD2. Therefore, anti-O-acetyl-GD2 antibodies might show higher tumor specificity and less adverse effects.

In summary, we have demonstrated that the combination of anti-GD2 mAbs and Vorinostat is highly effective in an orthotopic neuroblastoma mouse model. The combination not only demonstrated a significant growth inhibition but also significantly increased the survival of these mice. These results are encouraging, given that orthotopic models are more clinically relevant and better predictive of clinical drug efficacy than heterotopic models. Our findings underscore the potential clinical benefit of HDAC inhibition to reprogram the tumor microenvironment for subsequent improved response to immunotherapy. Importantly, anti-GD2 mAbs and Vorinostat are FDA approved and both are already clinically used in pediatric oncology. Our study therefore not only provides a strong rationale but the results may also be readily translated into clinical testing of anti-GD2 mAbs and Vorinostat immunocombination therapy in neuroblastoma patients.

Acknowledgments

We would like to thank Wenny Peeters, Jasper Lok, and Paul Rijken for their excellent technical assistance.

Disclosure statement

The authors declare no potential conflicts of interest.

Funding

This work was supported by the foundations "Villa Joep" and "Vrienden KOC Nijmegen".

ORCID

Louis Boon  <http://orcid.org/0000-0002-0937-9171>

Peter M. Hoogerbrugge  <http://orcid.org/0000-0003-3012-6109>

Gosse J Adema  <http://orcid.org/0000-0002-6750-1665>

References

1. Maris JM, Hogarty MD, Bagatell R, Cohn SL. Neuroblastoma. *Lancet*. 2007;369(9579):2106–2120. doi:10.1016/S0140-6736(07)60983-0.
2. Cheung NK, Dyer MA. Neuroblastoma: developmental biology, cancer genomics and immunotherapy. *Nat Rev Cancer*. 2013;13(6):397–411. doi:10.1038/nrc3526.
3. Svennerholm L, Boström K, Fredman P, Jungbjer B, Lekman A, Månsson JE, Rynmark BM. Gangliosides and allied glycosphingolipids in human peripheral nerve and spinal cord. *Biochim Biophys Acta*. 1994;1214(2):115–123. doi:10.1016/0005-2760(94)90034-5.
4. Mackall CL, Merchant MS, Fry TJ. Immune-based therapies for childhood cancer. *Nat Rev Clin Oncol*. 2014;11(12):693–703. doi:10.1038/nrclinonc.2014.177.
5. Cheever MA, Allison JP, Ferris AS, Finn OJ, Hastings BM, Hecht TT, Mellman I, Prindiville SA, Viner JL, Weiner LM, et al.

- The prioritization of cancer antigens: a national cancer institute pilot project for the acceleration of translational research. *Clin Cancer Res.* 2009;15(17):5323–5337. doi:10.1158/1078-0432.CCR-09-0737.
6. Cheung NK, Cheung IY, Kramer K, Modak S, Kuk D, Pandit-Taskar N, Chamberlain E, Ostrovskaya I, Kushner BH. Key role for myeloid cells: phase II results of anti-GD2 antibody 3F8 plus granulocyte-macrophage colony-stimulating factor for chemoresistant osteomedullary neuroblastoma. *Int J Cancer.* 2014;135(9):2199–2205. doi:10.1002/ijc.28851.
 7. Tarek N, Le Ludec J-B, Gallagher MM, Zheng J, Venstrom JM, Chamberlain E, Modak S, Heller G, Dupont B, Cheung NKV, et al. Unlicensed NK cells target neuroblastoma following anti-GD2 antibody treatment. *J Clin Invest.* 2012;122(9):3260–3270. doi:10.1172/JCI62749.
 8. Smith V, Foster J. High-risk neuroblastoma treatment review. *Children (Basel).* 2018;5(9):114.
 9. Yu AL, Gilman AL, Ozkaynak MF, London WB, Kreissman SG, Chen HX, Smith M, Anderson B, Villablanca JG, Matthay KK, et al. Anti-GD2 antibody with GM-CSF, interleukin-2, and isotretinoin for neuroblastoma. *N Engl J Med.* 2010;363(14):1324–1334. doi:10.1056/NEJMoa0911123.
 10. Matthay KK, Reynolds CP, Seeger RC, Shimada H, Adkins ES, Haas-Kogan D, Gerbing RB, London WB, Villablanca JG. Long-term results for children with high-risk neuroblastoma treated on a randomized trial of myeloablative therapy followed by 13-cis-retinoic acid: a children's oncology group study. *J Clin Oncol.* 2009;27(7):1007–1013. doi:10.1200/JCO.2007.13.8925.
 11. Lindau D, Gielen P, Kroesen M, Wesseling P, Adema GJ. The immunosuppressive tumour network: myeloid-derived suppressor cells, regulatory T cells and natural killer T cells. *Immunology.* 2013;138(2):105–115. doi:10.1111/imm.12036.
 12. Asgharzadeh S, Salo JA, Ji L, Oberthuer A, Fischer M, Berthold F, Hadjidaniel M, Liu CWY, Metelitsa LS, Pique-Regi R, et al. Clinical significance of tumor-associated inflammatory cells in metastatic neuroblastoma. *J Clin Oncol.* 2012;30(28):3525–3532. doi:10.1200/JCO.2011.40.9169.
 13. Kroesen M, Büll C, Gielen PR, Brok IC, Armandari I, Wassink M, Looman MWG, Boon L, den Brok MH, Hoogerbrugge PM, et al. Anti-GD2 mAb and Vorinostat synergize in the treatment of neuroblastoma. *Oncoimmunology.* 2016;5(6):e1164919. doi:10.1080/2162402X.2016.1164919.
 14. Liu YJ, Wang L, Predina J, Han R, Beier UH, Wang LCS, Kapoor V, Bhatti TR, Akimova T, Singhal S, et al. Inhibition of p300 impairs Foxp3(+) T regulatory cell function and promotes antitumor immunity. *Nat Med.* 2013;19(9):1173–1177. doi:10.1038/nm.3286.
 15. Condorelli F, Gnemmi I, Vallario A, Genazzani AA, Canonico PL. Inhibitors of histone deacetylase (HDAC) restore the p53 pathway in neuroblastoma cells. *Br J Pharmacol.* 2008;153(4):657–668. doi:10.1038/sj.bjp.0707608.
 16. Haberland M, Montgomery RL, Olson EN. The many roles of histone deacetylases in development and physiology: implications for disease and therapy. *Nat Rev Genet.* 2009;10(1):32–42. doi:10.1038/nrg2485.
 17. Jubierre L, Jiménez C, Rovira E, Soriano A, Sábado C, Gros L, Llorca A, Hladun R, Roma J, Toledo JSD, et al. Targeting of epigenetic regulators in neuroblastoma. *Exp Mol Med.* 2018;50(4):51. doi:10.1038/s12276-018-0077-2.
 18. Vo DD, Prins RM, Begley JL, Donahue TR, Morris LF, Bruhn KW, de la Rocha P, Yang M-Y, Mok S, Garban HJ, et al. Enhanced antitumor activity induced by adoptive T-cell transfer and adjunctive use of the histone deacetylase inhibitor LAQ824. *Cancer Res.* 2009;69(22):8693–8699. doi:10.1158/0008-5472.CAN-09-1456.
 19. Kroesen M, Nierkens S, Ansems M, Wassink M, Orentas RJ, Boon L, den Brok MH, Hoogerbrugge PM, Adema GJ. A transplantable TH-MYCIN transgenic tumor model in C57Bl/6 mice for preclinical immunological studies in neuroblastoma. *Int J Cancer.* 2014;134(6):1335–1345. doi:10.1002/ijc.28463.
 20. van den Bijgaart RJE, Kroesen M, Wassink M, Brok IC, Kers-Rebel ED, Boon L, Heise T, van Scherpenzeel M, Lefeber DJ, Boltje TJ, et al. Combined sialic acid and histone deacetylase (HDAC) inhibitor treatment up-regulates the neuroblastoma antigen GD2. *J Biol Chem.* 2019;294(12):4437–4449. doi:10.1074/jbc.RA118.002763.
 21. Kroesen M, Brok IC, Reijnen D, van Hout-kuijper MA, Zeelenberg IS, Den Brok MH, Hoogerbrugge PM, Adema GJ. Intra-adrenal murine TH-MYCIN neuroblastoma tumors grow more aggressive and exhibit a distinct tumor microenvironment relative to their subcutaneous equivalents. *Cancer Immunol Immunother.* 2015;64(5):563–572. doi:10.1007/s00262-015-1663-y.
 22. Mujoo K, Kipps TJ, Yang HM, Cheresch DA, Wargalla U, Sander DJ, Reisfeld RA. Functional properties and effect on growth suppression of human neuroblastoma tumors by isotype switch variants of monoclonal antiganglioside GD2 antibody 14.18. *Cancer Res.* 1989;49(11):2857–2861.
 23. Hegde PS, Chen DS. Top 10 Challenges in Cancer Immunotherapy. *Immunity.* 2020;52(1):17–35. doi:10.1016/j.immuni.2019.12.011.
 24. Schmulde M, Friebe E, Sonnemann J, Beck JF, Bröker BM. Histone deacetylase inhibitors prevent activation of tumour-reactive NK cells and T cells but do not interfere with their cytolytic effector functions. *Cancer Lett.* 2010;295(2):173–181. doi:10.1016/j.canlet.2010.02.024.
 25. Cassetta L, Bækkevold ES, Brandau S, Bujko A, Cassatella MA, Dorhoi A, Krieg C, Lin A, Loré K, Marini O, et al. Deciphering myeloid-derived suppressor cells: isolation and markers in humans, mice and non-human primates. *Cancer Immunol Immunother.* 2019;68(4):687–697. doi:10.1007/s00262-019-02302-2.
 26. Kramer K, Gerald WL, Kushner BH, Larson SM, Hameed M, Cheung NK. Disialoganglioside G(D2) loss following monoclonal antibody therapy is rare in neuroblastoma. *Clin Cancer Res.* 1998;4(9):2135–2139.
 27. Kramer K, Gerald WL, Kushner BH, Larson SM, Hameed M, Cheung NK. Disialoganglioside GD2 loss following monoclonal antibody therapy is rare in neuroblastoma. *Med Pediatr Oncol.* 2001;36(1):194–196. doi:10.1002/1096-911X(20010101)36:1<194::AID-MPO1046>3.0.CO;2-B.
 28. Pollard JW. Tumour-educated macrophages promote tumour progression and metastasis. *Nat Rev Cancer.* 2004;4(1):71–78. doi:10.1038/nrc1256.
 29. Guerriero JL, Sotayo A, Ponichtera HE, Castrillon JA, Pourzia AL, Schad S, Johnson SF, Carrasco RD, Lazo S, Bronson RT, et al. Class IIa HDAC inhibition reduces breast tumours and metastases through anti-tumour macrophages. *Nature.* 2017;543(7645):428–432. doi:10.1038/nature21409.
 30. Shusterman S, London WB, Gillies SD, Hank JA, Voss SD, Seeger RC, Reynolds CP, Kimball J, Albertini MR, Wagner B, et al. Antitumor activity of hu14.18-IL2 in patients with relapsed/refractory neuroblastoma: a Children's Oncology Group (COG) phase II study. *J Clin Oncol.* 2010;28(33):4969–4975. doi:10.1200/JCO.2009.27.8861.
 31. Navid F, Santana VM, Barfield RC. Anti-GD2 antibody therapy for GD2-expressing tumors. *Curr Cancer Drug Targets.* 2010;10(2):200–209. doi:10.2174/156800910791054167.
 32. Kushner BH, Cheung IY, Modak S, Kramer K, Ragupathi G, Cheung NKV. Phase I trial of a bivalent gangliosides vaccine in combination with beta-glucan for high-risk neuroblastoma in second or later remission. *Clin Cancer Res.* 2014;20(5):1375–1382. doi:10.1158/1078-0432.CCR-13-1012.
 33. Louis CU, Savoldo B, Dotti G, Pule M, Yvon E, Myers GD, Rossig C, Russell HV, Diouf O, Liu E, et al. Antitumor activity and long-term fate of chimeric antigen receptor-positive T cells in patients with neuroblastoma. *Blood.* 2011;118(23):6050–6056. doi:10.1182/blood-2011-05-354449.
 34. Alvarez-Rueda N, Desselle A, Cochonneau D, Chaumette T, Clemenceau B, Leprieux S, Bougras G, Supiot S, Mussini J-M, Barbet J, et al. A monoclonal antibody to O-acetyl-GD2 ganglioside and not to GD2 shows potent anti-tumor activity without peripheral nervous system cross-reactivity. *PLoS One.* 2011;6(9):e25220. doi:10.1371/journal.pone.0025220.